تقييم كفاءة وحدة تحلية المياه بالأغشية المدعمة
بطاقة الرياح في المملكة العربية السعودية

عماد علي ، مراد بو معزه وعبد الحميد أجبار

قسم الهندسة الكيميائية، جامعة الملك سعود، الرياض، المملكة العربية السعودية

الخـــلاصـــة

المملكة العربية السعودية دولة صحراوية تواجه تحديات متواصلة لتوفير متطلبات مياه الشرب المتزايدة بسبب تنامي عدد السكان ونمو القطاع الصناعي. وحاليا يتم توفير أكثر من نصف احتياجات مياه الشرب في المملكة من محطات تحلية مياه البحر والمياه الجوفية. وبالرغم من أن السعودية دولة ثرية نفطيا إلا أن تحلية المياه تمثل عبئا اقتصاديا لارتفاع تكلفتها. كما أن تحلية المياه الحرارية ذات تأثير سلبي على البيئة. لذا أصبح من الضروري البحث عن مصادر طاقة بديلة أقل تكلفة وأقل ضررا على البيئة لتوفير محطات تحلية مياه اقتصادية. وتعتبر طاقة الرياح مصدرا مستحبا لاستخدامه في عمليات تحلية المياه المالحة. تهدف هذه الدراسة لاستكشاف جدوى استخدام طاقة الرياح المتوفرة في المنطقة الشرقية من البلاد لإنتاج مياه محلاة باستخدام وحدات التناضح العكسي لتحلية المياه المالحة. وقد أوضحت الدراسة قدرة طاقة الرياح المتوفرة على تشغيل وحدات تحليه بالتناضح العكسي بمواصفات قياسية مقبولة، حيث انه بالإمكان تشغيل وحدتي تناضح عكسي مدعمة بوحدة استرجاع للطاقة لإنتاج مياه محلاه بقدرة استخلاص تصل الى 60% من المياه المالحة وبطاقة استهلاكيه تتراوح بين 0.5 الى 2 كيلو وات ساعة لكل متر مكعب. كما انه بالإمكان تشغيل تلك الوحدات بنفس الكفاءة حتى في تواجد تقلبات طفيفة في طاقة الرياح.

Performance assessment of a wind driven membrane desalination unit in Saudi Arabia

Emad Ali, Mourad Boumaza and Abdelhamid Ajbar
Chemical Engineering Department, King Saud University, Riyadh, Saudi Arabia

ABSTRACT

Situated in a mostly desert area, the kingdom of Saudi Arabia (KSA) faces the continuous challenge of satisfying water needs of its growing population and industry. Currently, sea or brackish water desalination plants satisfy more than half of the water demands of the kingdom. However, even with the country being an oil producer, desalination is an energy intensive industry making the investment in this field a costly process. Thermal desalination plants are also large pollutants. Therefore, cheaper and cleaner alternative sources of power are required to provide lower cost desalination solutions. Wind power is an attractive option to be utilised with desalination technologies. This paper investigates the potential utilization of wind energy to drive a reverse osmosis (RO) desalination unit to produce fresh water from brackish water in the Saudi Arabian gulf region. The analysis proved the capability of existing wind power to operate RO desalination units within acceptable performance standards. For a two stages process with an energy recovery device, 60% recovery rate can be achieved and the energy consumption can be kept within 0.5~2 kWh/m3 based on the local available wind power. An acceptable RO operation can be efficient in the presence of mild fluctuations in wind power.

INTRODUCTION

Water is a valuable natural resource and its shortage represents a serious problem being faced in many areas of the planet. Decision making on the water supply method includes technical and economic evaluation of various alternatives, considering the urgent character of the problem and the need for its sustainable solution. Desalination of brackish water (Vlachos & Kaldellis, 2004) and sea water (Kaldellis et al., 2000) is known to have the potential to meet water demand in areas with limited water resources. However, a critical issue in the viability of water desalination technologies has always been its high-energy consumption coupled with its negative environmental impact. Among the various existing technologies, desalination based on reverse osmosis (RO) requires the lowest energy. Typically 3 to 6kWh of electric power is required for the extraction of one cubic meter of freshwater from seawater (Dashtpour & Al-Zubaidy, 2012).The major fraction of energy is used to pressurize the feed water. However, the cost of produced water is sensitive to fossil fuel prices. Charcosset (2009) estimated that a 25% variation in energy cost can lead to an 11% change in the cost of produced water. These cost fluctuations can be avoided, if the system is operated with renewable energy sources (RES). For this reason, hybrid systems in which solar or wind energy is coupled with the RO desalination system are attracting increasing attention.

Saudi Arabia is a rapidly developing country and the demand for electricity for multiple purposes (air conditioning and desalination units) is growing around 5% annually. The state power grid system supplies electricity to approximately 80% of the population living in the state capital and industrial centres. Given the country's large surface area (2.3 million km2), the power grid system cannot cover economically all the remote regions. Hence many remote and sparsely populated communities are in need of not only an independent source of power, but they also need fresh water. These communities represent a real potential for the application of renewable energy to generate electric power and to operate small RO desalination units for the production of fresh water from underground brackish water. Because of its desert climate, it is normal that extensive research studies have investigated the use of solar energy to generate electric power that could be used to support national grid and/or to be used to power RO desalination units in remote areas. The study of the use of wind energy, which is the purpose of this paper, has however not attracted similar attention.

In other parts of the world, extensive research was carried out on the utilization of wind energy to run RO units. Miranda & Infield (2002), for example, studied the use of a small-scale wind-powered RO system for seawater desalination. The system included an energy recovery device to support its usage in islands or isolated inland areas. The system's performance over wide operating conditions was investigated. Thomson et al. (2002) proposed an energy recovery by Clark pump to reduce the specific energy for seawater desalination to less than 3.5 kWh/m3. The system operated without the need for energy storage. Pestana et al. (2004) performed an experimental study on an RO plant operated by wind energy and energy storage. The plant could function over a wide range of operating conditions with respect to available power. Park et al. (2011) studied the effect of wind power variations on the performance of RO system for brackish water desalination. The investigation showed the ability of the proposed system to handle wind speed fluctuations at low feed salinity. At high salt feed concentration, adequate control strategy was required to maintain good-quality product. Carta et al. (2004), on the other hand, described the design and operation strategies for a stand-alone wind-powered desalination system. It was found that RO technology outperforms the electro dialysis reversal technology and vacuum vapour compression technology, when used with wind farms that were isolated from conventional energy grid. Per our knowledge, little work has been done to study the performance of RO desalination system for brackish water using wind power as the only source of energy. Moreover, energy recovery devices are not widely used in brackish water RO systems (Sessions et al., 2011). This paper studies a scheme for the production of fresh water from wells in the eastern part (Dahran province) of this country. The scheme consists of stand-alone wind turbine powering a reverse osmosis unit. The scheme is also equipped with an energy recovery device (ERD). The objectives of this work are not only to understand and assess the wind-powered RO system behaviour, but also to evaluate the process performance over different operating conditions.

WIND ENERGY DATA

A number of studies were carried out to evaluate the potential use of wind energy in Saudi Arabia. Data for wind in 20 locations in Saudi Arabia have been analysed (Rehman et al., 2003). According to Martin (1985), winds in these locations have a speed ranging from 2.5 (Bisha district) to 4.4 m/s (Dahran district), and a power ranging from 21.8 to 77.7 W/m2. These data indicate that wind power could be more profitable with small-scale uses. Wind speed data are also available from the Meteorology and Environment Protection Administration (MEPA) (Fath et al., 2013). The wind map of Saudi Arabia (Rehman et al., 2003; Khonkar, 2009) indicates the availability of two large regions of wind along the Red Sea and Arabian Gulf coastal areas. The speed for wind ranges from 14 to 22 kmph in the Arabian gulf and from 16 to 19 kmph over the red sea coastal areas. Moreover, Rehman (2006) reported four sites that can be used for possible utilization of wind energy. These locations are Al-Wajh and Yenbo on the coast of Red Sea, Quaisumah in the north east and Dahran on the Arabian gulf coast.

In this paper, the data obtained from the Saudi Arabian Presidency of Meteorology and Environment, covering the last three decades have been analysed. Figure 1 shows the monthly average wind speed for the period of 1978-2007 for three regions: Dahran (east coast), Riyadh (center) and Jeddah (west coast). The data for Dahran area shows the highest wind speed with a monthly average of 4.5 m/s, and it is for this purpose that this paper investigates the possible use of wind energy to drive an RO plant located in the Dahran region.
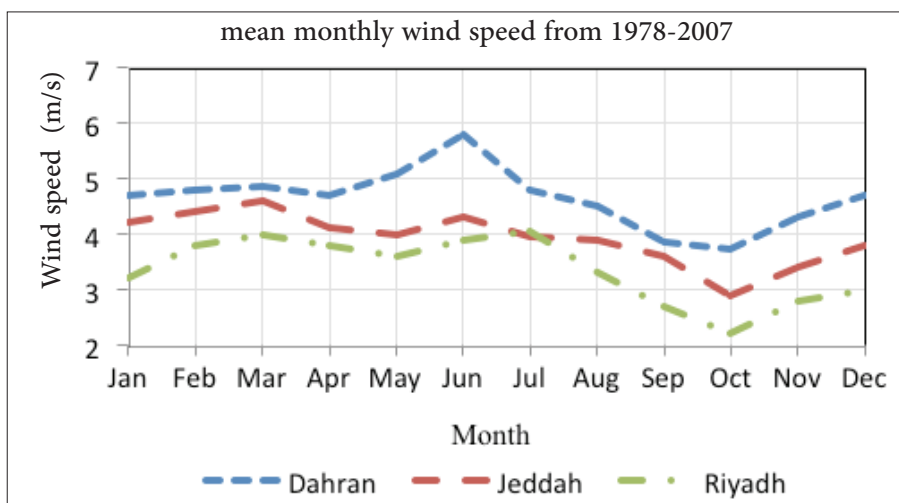

Fig.1. Monthly wind speed for three Saudi regions [4]

PROCESS DESCRIPTION AND MODELLING

The proposed system consists of a two-stage RO desalination unit powered directly by wind turbine with energy recovery and the possibility of inter-stage pumping that boosts the pressure in the second stage. The system is illustrated in Figure 2. Usually, the brine exiting the first stage is at high pressure, thus it can be used to power a second stage. Therefore, an additional amount of permeate can be produced in the second stage and consequently increasing the overall water recovery. This achievement can be done without the need for further increase in the feed pressure.

The main design features of this Energy Recovery Device (ERD) dual work exchanger energy recovery (DWEER) system is to recover energy from the high pressure brine stream, since the pressure drop across the RO membrane is usually low i.e. the typical pressure drop in membrane channel for brackish water is 1.0 bar (DOW, 2006). Another design feature is the incorporation of a pump either between the two stages or in the recycled feed flow rate. The purpose of the inter-stage pump is to increase the brine pressure before entering the second stage. The outlet brine from the second stage will be high enough such that DWEER can maintain the makeup feed pressure to the desired main feed pressure and thus eliminating the need for a post-DWEER booster pump. Alternatively, a feed boost pump can be used after the DWEER to adjust the pressure of makeup feed. The makeup feed recovers energy from the DWEER, but it might be less than the main feed to the RO unit. In this case, the boost pump will compensate the difference. The pressure and volume flow are controlled by means of a regulating device and adapted to the given operating conditions. A storage battery maintains the brief and temporary compensation for variations in the system load. Furthermore, a water storage system is connected to the plant to ensure the continuation of operation in cases of lower wind energy.
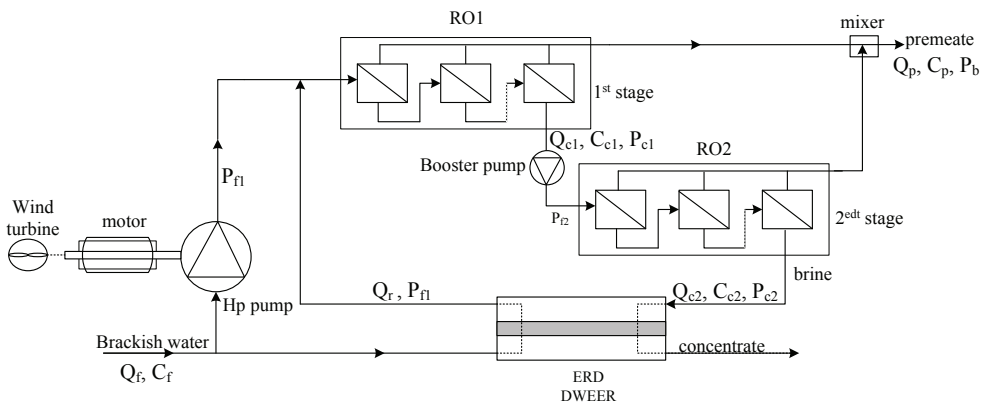

Fig. 2. Schematic of the wind-driven RO system with DWEER and inter-stage booster pump

Wind turbine energy output.

For the purpose of determining the average power of a turbine over a range of wind speeds, a probability density distribution is required. The law of Weibull statistical distribution appears to be a good candidate to describe the wind speed with a reasonable good fit to wind data. The probability density function is given by Lagomarsino et al. (1992):

$$f(V) = \left(\frac{k}{C}\right)\left(\frac{V}{C}\right)^{k-1} \exp\left[-\left(\frac{V}{C}\right)^{k}\right]$$

(1)

C and k are parameters, which are called respectively the scale factor (m/sec) and the shape factor (dimensionless) are used to fit the distribution. Generally, the average wind speed for a specific region is recorded at a standard height (10 m a.s.l). In order to determine the wind speed for different heights, the following modified power law (Justus & Mikhail, 1976), has been used:

$$C_2 = C_1 \cdot \left(\frac{Z_2}{Z_1}\right)^m \tag{2}$$

$$k_2 = \frac{k_1}{\left[1 - 0.0881 \times \ln\left(\frac{Z_2}{Z_1}\right)\right]} \tag{3}$$

The exponent, m, depends on the roughness, Z0, and the geometric height, Z, and is provided by:

$$m = \frac{1}{\ln(Z/Z_0)} - 0.0881 \times \ln\left(\frac{C_1}{6}\right) \tag{4}$$

Where:

$$Z = \sqrt{Z_1 . Z_2} \tag{5}$$

The average annual power output of a wind turbine is a very important parameter, since it determines the total energy production and the total income. It can be evaluated by using the following relation (Poje & Cividini, 1988):

$$\bar{P} = \int_0^\infty P(V).f(V).dV \tag{6}$$

Several models are available in the literature to predict the power provided by wind turbines as function of the wind speed. Based on Figure 3, all these models consider that the power is zero, when the wind speed is either below the cut-in speed V1(region 1) or above the cur-out speed, Vo (region 4) while the power remains approximately constant between the rated-output speed VR and Vo (region 3). For the interval V1<V<VR, the power obtained from the wind turbine can be estimated by a mathematical model. There are no specific reliable models, which can be valid for all wind turbines. However, according to several published works, the quadratic model seems to be the most appropriate to predict power as a function of wind speed, as it provides the least error margin. Practically, the cut-in speed, V1 is typically between 3 and 4 m/s, the rated-output speed VR is typically between 12 and 17 m/s and the cur-out speed, Vo is typically around 25 m/s (Wind power program.com).
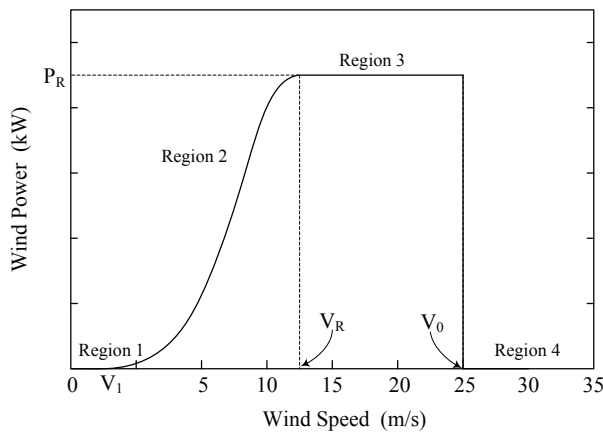

Fig. 3. Typical wind turbine power output with steady wind speed

The steady power P(V) is expressed as follows:

$$P(V) = \begin{cases} 0 & if & V < V_1 \\ \alpha + \beta V + \gamma V^2 & if & V_1 \le V < V_R \\ P_R & if & V_R < V \le V_0 \\ 0 & if & V > V_0 \end{cases} \tag{7}$$

The constants α, β and γ are then extracted by the following relations (Zimmer et al., 1975; Chou & Corotis, 1981):

$$\begin{cases} \alpha + \beta V_1 + \gamma V_1^2 = 0 \\ \alpha + \beta V_R + \gamma V_R^2 = P_R \\ \alpha + \beta V_c + \gamma V_c^2 = P_R \left(\dfrac{V_c}{V_1}\right)^3 \end{cases} \tag{8}$$

Where $V_c = (V_c + V_1)/2$.

The third equation is in fact an empirical one and was proposed by Zimmer et al. (1975) in order to produce realistic curves for the power distribution. Equation (6) can be then expressed as follows:

$$\bar{P} = \int_{V_1}^{V_0} \left(\alpha + \beta V + \gamma V^2\right) \frac{k_1}{C_1} \left(\frac{V}{C_1}\right)^{k_1-1} \exp\left[-\left(\frac{V}{C_1}\right)^{k_1}\right] + P_R \left\{\exp\left[-\left(\frac{V_R}{C_1}\right)^{k_1}\right] - \exp\left[-\left(\frac{V_0}{C_1}\right)^{k_1}\right]\right\} \tag{9}$$

The capacity factor is an important index to evaluate the performance of a wind turbine. It is defined as the ratio of the annual average power, to the hypothetical maximum possible, i.e.

$$CF = \frac{\bar{P}}{P_R} \tag{10}$$

Table 1. Wind turbine parameters

Item	Value
Rated power (kW)	1000
Rotor diameter (m)	54
Hub height (m)	70.82
Swept area of rotor (m²)	2290
Cut-in wind speed (m/s)	3
Cut-out wind speed (m/s)	20
Rated wind speed (m/s)	16
Rotor speed (rpm)	15 – 22
Tower type	Tubular

The wind turbine-related parameters considered in this study are summarized in Table 1, while Figure 4 presents the effect of the wind speed on the available power based on a rated output power of 1MW. Considering a steady average wind speed of 4.5 m/s in Dahran region (Figure 1), the available wind power is therefore around 100 kW.
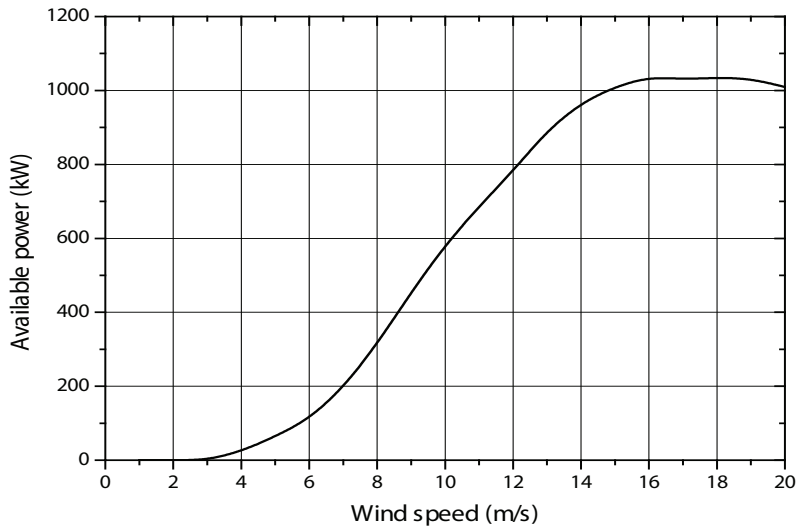
Fig.4. Power curve of the 1MW rated wind turbine

RO Desalination unit production

The equations, at steady state, relative to the transport of solute and solvent are provided by Marriott & Sorensen (2003):

$$Q_f = Q_p + Q_c$$

$$Q_f C_f = Q_p C_p + Q_c C_c \tag{11}$$

The solvent volumetric flux, J_w, is given by Vincea et al. (2008):

$$J_w = A(T)(\Delta P - \Delta \pi) \tag{12}$$

while the mass flux, Js, of the solute is given by:

$$J_s = B(T)\left(C_m - C_p\right) \tag{13}$$

When the concentration polarization is present, the flux, Jw, at steady state, is given by Sherwood & Brian (1967):

$$J_w = k_s \ln \frac{C_m - C_p}{C_b - C_p} \tag{14}$$

In Equation (12), we use the following correlation for pressure drop (Vincea et al., 2008):

$$\Delta P = P_f - P_b - P_{drop/2}$$

$$\Delta \pi = b_m (C_m - C_p) \tag{15}$$

The solute flux is used to determine the osmotic pressure across the membrane, as follows;

$$J_s = J_w C_p \tag{16}$$

The combination of Equations (14) – (16) and the elimination of Cm allows to obtain the following expression for the flux (Rautenbach, 1986):

$$J_w = A(T) \left[\Delta P - b_\pi \left(\frac{B(T)C_b \exp(J_w/k_s)}{J_w + B(T)\exp(J_w/k_s)} \right) \exp(J_w/k_s) \right] \tag{17}$$

and

$$C_p = \frac{B(T)C_b}{B(T) + J_w \exp(J_w/k_s)} \tag{18}$$

Once the nonlinear algebraic Equation (17) is numerically solved, the permeate concentration, Cp, can be calculated using Equation. (18). Also, we constraint this concentration to be smaller than a desired specific value, Cpd:

$$C_p \le C_{pd} \tag{19}$$

The dependence on the temperature of the water permeability, A(T), of the membrane and the permeability, B(T), of membrane salts are provided by the following correlations (Sarkar et al., 2008):

$$A(T) = A_0 \frac{\mu(T_0)}{\mu(T)} \tag{20}$$

$$B(T) = B_0 \times \frac{T}{T_0} \times \frac{\mu_0}{\mu(T)} \tag{21}$$

The viscosity μ(T), can be calculated by the Guzman–Andrade equation (Agashichev, 2005):

$$\mu(T) = \alpha \exp\left(\frac{b}{T}\right) \tag{22}$$

Where the values of α and b can be calculated from the available correlations (Perry & Green, 1985. The recovery rate (R) and Salt rejection (SR) are the selected parameters to asses the performance of the RO. They are defined :

$$R = Q_p / Q_f \tag{23}$$

$$SR = 1 - \frac{C_p}{C_b} \tag{24}$$

$$SP = 1 - SR = C_p / C_b \tag{25}$$

Perforated baffles are used in spiral-wound membrane modules, since they increase mass transfer. The following equation can be used to determine the mass transfer coefficient, ks (Costa et al., 1994):

$$Sh = 0.065 Re^{0.865} Sc^{0.25} \tag{26}$$

where

$$Sh = \frac{k_s}{D_{AB}}; Re = \frac{d_h u}{\mu}; Sc = \frac{\square}{D_{AB}} \tag{27}$$

A spiral wound module hydraulic diameter depends on the specific surface area of the spacer, the void fraction and the channel height. Table 2 shows the membrane specifications (Al-Bastaki & Abbas, 2003), while Table 3 presents the physical characteristics of the untreated water.

Table 2. Geometric specification of membrane module (Al-Bastaki & Abbas, 2003)

Parameter	Value
Hydraulic diameter of channel, d_h (mm)	0.78045
Height of spacer channel, h_{sp} (mm)	0.593
void fraction of the spacer, ε (porosity)	0.9
Length of membrane, L (m)	1
Width of membrane, W (m)	37
Active area of the membrane, A_e (m²)	37
Reference water permeability, A_0 (m³/h.bar)	19.43×10^{-4}
Reference solute permeability, B_0 (m³/h)	$78,55 \times 10^{-5}$

The velocity in the feed channel that contains baffle is given by:

$$u = \frac{Q_f}{w h \varepsilon} \tag{28}$$

dh, hsp and ε are the baffle parameters. The flow rate of bulk fluid and its concentration are given by:

$$Q_b = \frac{Q_f + Q_c}{2} \tag{29}$$

$$C_b = \frac{C_f + C_c}{2} \tag{30}$$

The kinematic viscosity, v, for brackish water can be calculated through following correlation (Sourirajan, 1970):

$$v = 0.0032 + 3.0 \times 10^{-6} C_b + 4.0 \times 10^{-9} C_b^2 \tag{31}$$

The value of diffusivity, DAB, is estimated to be 5.5×10-6 m2/h. Therefore, the osmotic coefficient, $b\pi$, is:

$$b_\pi = \pi / C_b \tag{32}$$

The osmotic pressure, v, is calculated using following relationship:

$$\pi = 1{,}12T \sum \bar{m}_i \tag{33}$$

Where $\sum \bar{m}_i$ is the sum of all molalities of dissolved ions (ppm).

The energy needed to pressurize the feed stream is given by:

$$E_p = Q_f P_f / \eta_p \tag{34}$$

The power that is recovered by the ERD is:

$$E_{ERD} = Q_c P_c \eta_{ERD} \tag{35}$$

The water pressure on the concentrate side is:

$$P_c = \Delta P - P_{drop} \tag{36}$$

The pressure drop, P_{drop}, is given by the following correlation (Vince et al., 2008):

$$P_{drop} = \lambda \left(\frac{Q_f + Q_c}{2 \times 3600} \right)^a \tag{37}$$

In Equation (37) l = 9.5x108 and a = 1.7. The water flow rate pumped by the wind turbine is given by (Zejli et al., 2010):

$$Q_f = \frac{3600 \times P_w}{P_f \eta_p^{-1} - (P_f - P_{drop})(1 - R) Q_f \eta_{ERD}} \tag{38}$$

The specific energy required for the generation of 1 m3 of freshwater is provided by Park et al. (2011):

$$E = \frac{Q_f P_f \eta_p^{-1} - Q_c P_c \eta_{ERD}}{Q_p} \tag{39}$$

Solution methodology

To understand the methodology for solving the RO model equations, a flow chart describing the main steps is shown in Figure 5. The system has a degree of freedom of 3. Therefore, three variables must be fixed to solve the set of model equations. For example, as shown by the algorithm, R and Cp can be fixed to determine the necessary feed pressure to satisfy these fixed performance specifications. Initial value for Pf can be set to evaluate Qf using Equation 38. Afterward, the model equations are solved repeatedly over different values for Pf until the desired product quality is achieved. This approach is commonly used in the design stage to optimize the hydrostatic pressure for the desired process operation. Alternatively, Pf can be considered fixed based on previous design analysis. Hence, one can also fix R, calculate Qf and solve the model equations without iterations to determine Cp. The algorithm for this approach is not shown for space limitations. Regardless of the algorithm used, another internal iteration is conducted to determine the membrane wall concentration, Cm and water flux Jw. Usually these variables cannot be pre-specified, as they are not measurable and vary with feed specifications and operating conditions.
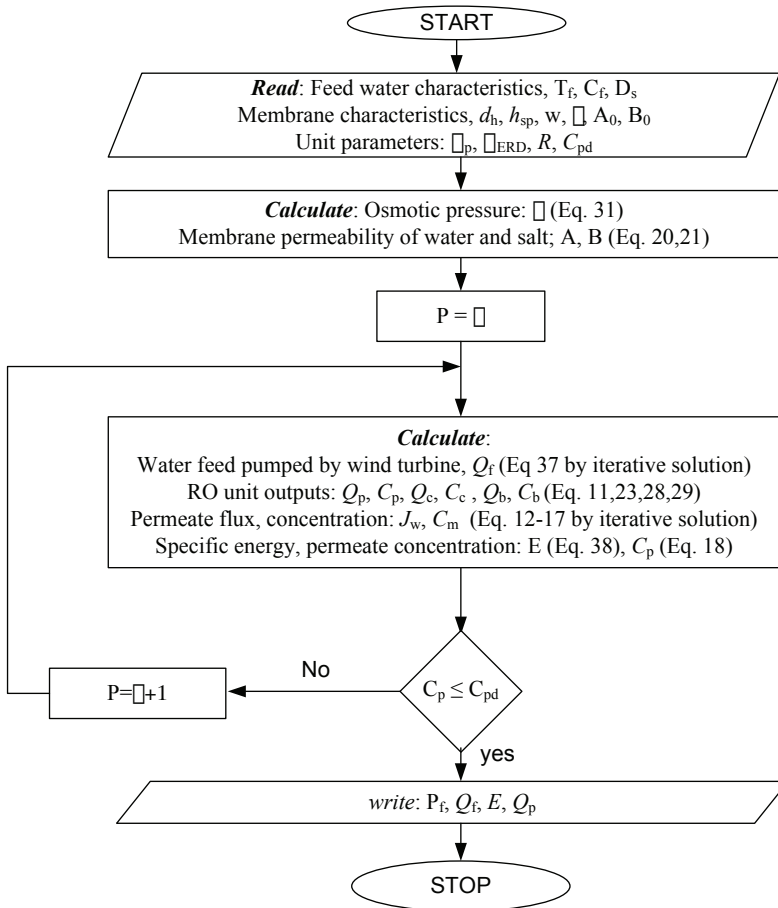

Fig. 5. Flow chart for RO model solution methodology

RESULTS AND DISCUSSION
Wind-driven feed pump

The data obtained for the Dahran Region was analyzed to determine the different operating parameters required for a membrane desalination plant using wind energy for a specific power, which in this case equals 100 kW. We have considered the wind turbine capacity factor (efficiency) to be 36%. First we study the performance of the wind-powered feed pump independently of the RO system. The analysis is obtained by solving Equation (38). The results which show the relationship between the expected feed flow rate and feed pressure is depicted in Figure 6 for a fixed turbine power of 100 kW, which corresponds to a wind speed of 4.5 m/s. The figure shows the pressure-flow diagram, when DWEER is not used and when DWEER is employed at two recovery ratios, namely 40 and 80%. For the given turbine power, the feed flow rate for all cases is limited between 20 and 350 m3/h and is inversely proportional to the feed pressure. Therefore, in order to operate the RO at high throughput, low pressure can be employed, which will sacrifice the RO performance in term of salt rejection. Incorporation of DWEER has a little effect on the overall power capacity of the system. This effect diminishes as the recovery ratio increases. This is obvious because as the recovery ratio increases, the flow rate of the brine decreases and so its associated energy. It is important to note, per Figure 6, that the available wind energy can operate the main pump at a wide range of pressures that span the required trans-membrane pressure for a typical RO element. The operational limit for an RO unit used in seawater desalination is 82 bar, while it is 41 bar for brackish water desalination (Vincea et al., 2008). Moreover, the generated flow rate is sufficient to operate common RO systems. Recalling that the maximum allowable feed flow rate for a single RO element is 1.4~4 m3/h, (DOW, 2006), the available flow rate is enough to operate a pressure vessel equipped with 10~100 RO elements.
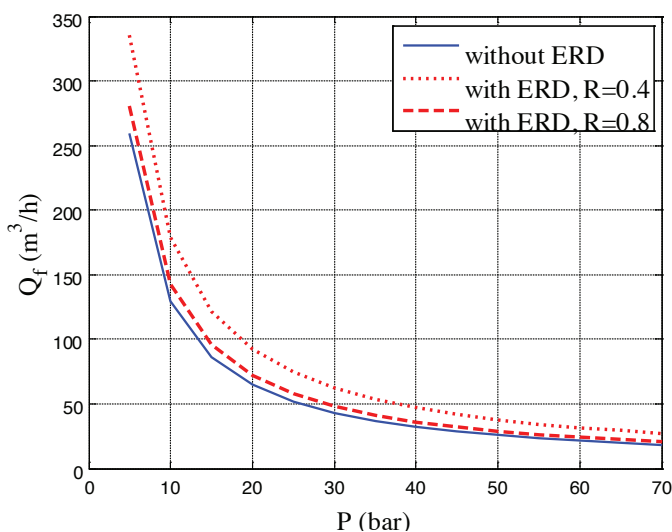

Fig. 6. Pressure versus Flow rate generated by the 100 kW wind turbine

Single stage RO system

The second analysis investigates the estimation of the input-output characteristic of a single stage RO system as shown in Figure 7. This system is a special case of that shown in Figure 2, where the brine outlet from the first stage is recycled to power the DWEER in order to adjust the makeup feed pressure. No booster pump is used. In general, the flow rate of the makeup feed is fixed; therefore, a booster pump is needed, when the recycled brine has not enough pressure to power up the DWEER. In our case, we consider the makeup feed flow rate to be variable so that its pressure can be maintained at the desired value of Pf in any case. In due course, the variations in the brine energy are reflected on the value of the specific energy, E computed by Equation (39).
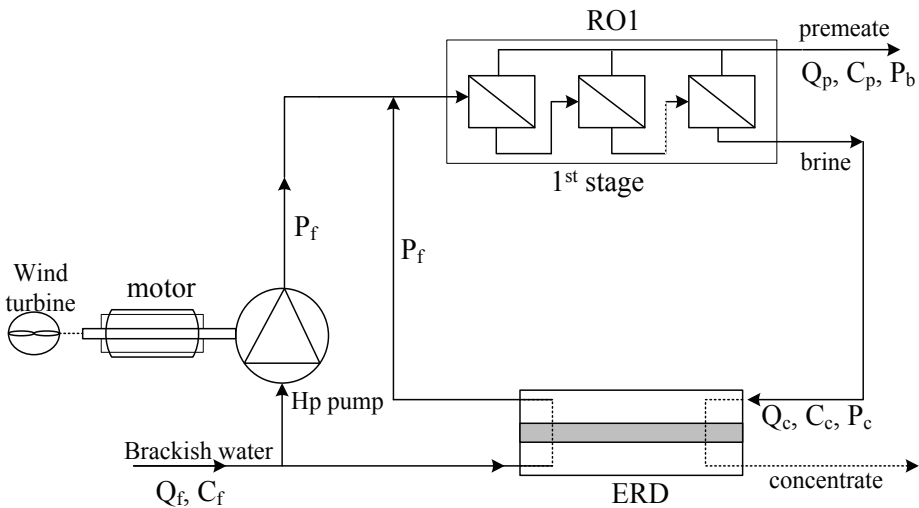

Fig. 7. Schematic of single stage wind-driven RO system

This performance analysis of the single stage system is obtained by solving the model equations according to the algorithm of Figure 5. The algorithm is solved for a desired permeate concentration of 0.26 kg/m3 and several values of the recovery rate. The result is shown in Figure 8. It is obvious that operating the RO system at high recovery percentage requires high feed pressure. Because of the correlation between the feed pressure and flow rate as shown earlier, the increasing pressure demand will limit the amount of brackish water that can be processed at high recovery ratios. Typically, the permeate production increases as the recovery increases, but as the feed flow rate declines, the permeate production reaches a maximum of 120 m3/h around 50% recovery. Similarly, the specific energy increases with feed pressure, but because of the convex profile of the permeate production, the specific energy reaches a minimum value of 1 kW/(m3/h) around 50% recovery. In order to achieve 80% recovery rate, high operating pressures exceeding 15 bar are required. Our simulation indicated that operating the RO system beyond 80% recovery factor is not possible. To operate the unit at elevated recovery ratio, high trans-membrane pressure is required, which because of the pressure-flow relationship, results in low feed flow rate. At low feed flow rate, the salt concentration at membrane wall builds up and so is the osmotic pressure thus weakening the water

flux across the membrane. To overcome such situation, higher feed pressure is needed to surpass the growing osmotic pressure, which will further reduce the feed flow rate. In fact, an operational limit of 70-80% for water recovery was reported for RO elements used in brackish water desalination (Greenlee et al., 2009).
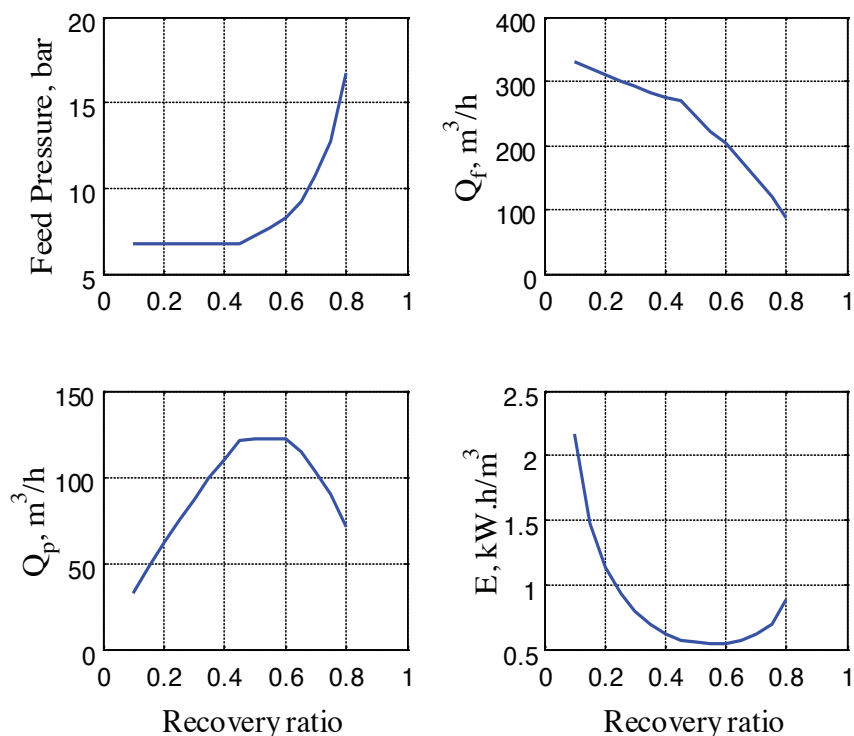
Fig. 8. Performance of a single stage RO system, hp = 0.6, hERD = 0.9, Cpd = 0.26 kg/m3

To further analyze and understand the system performance and limitation, we re-simulate the system at fixed pressure and recovery ratio, while the permeate concentration is allowed to vary. In this case, the algorithm of Figure 5 is carried out with minor modification as mentioned earlier, e.g. the pressure is fixed instead of being variable, while Equations (11-28) are solved simultaneously. The outcome of this simulation is depicted in Figure 9. Pressurizing the RO membrane decreases the feed flow rate according to the relationship outlined in Figure 6. This also decreases the permeate flow rate, because the recovery ratio is fixed at 80%. Intuitively, the energy consumption grows considerably. However, elevated hydrostatic pressure improves the salt rejection capability, because the driving force for mass transfer improves at high feed pressure. It should be noted, that rapid enhancement in salt rejection occurs below 15 bar afterward the rejection rate increases marginally, because at elevated salt reject, the salinity of the concentrate increases considerably. Moreover, at elevated membrane pressure, salt may dissolve in water and migrate through the membrane pores. Therefore, it is recommended to operate at 15 bar, where salt rejection is higher than 90% and

energy consumption per unit production is less than 1 kWh/m3. Furthermore, in order to operate the process at 80% recovery rate, high pressure is needed; otherwise low product quality will be produced as the salinity increases rapidly, when the pressure is less than 15 bar. Once again, our simulations revealed un-successful operation, when the feed pressure exceeds 35 bar. It is believed that there is a limit to the salt that can be extracted through the increase in feed pressure. Beyond that some salt dissolves and flows inside the membrane (Clayton et al., 2011). Moreover, depending on the feed conditions and the type of RO membrane, a maximum feed pressure of 41 bar (Vincea et al., 2008) and 27 bar (Srivathsan, 2013) are reported, when an RO element is used in brackish water desalination.
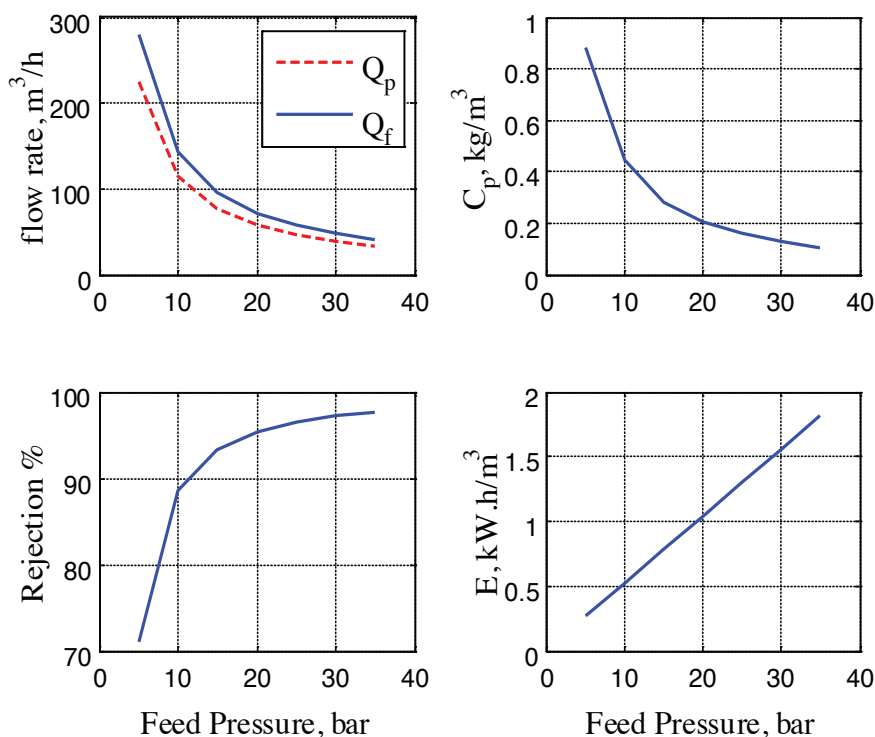

Fig. 9. Performance of a single stage RO system at R = 80% ,hp = 0.6, hERD = 0.9.

Two-stage RO system without a booster pump

The previous simulations indicate an economically optimal operation occurring at 40% recovery ratio. Hence there is potential to further enhance the overall performance by the addition of a second stage to utilize the pressure associated with the brine outlet from the first stage. The two- stage system is shown in Figure 2, but no booster pump is implemented for the same argument mentioned earlier. Simulation of this system is achieved by solving the first stage using the algorithm depicted in Figure 5 and the second stage using the same approach used to generate Figure 9. In fact, the feed pressure to second stage is fixed and equals the brine pressure exiting the first stage, while the performance specification i.e. salt rejection rate is set free and the water recovery can be set arbitrary. It should be noted that the main feed flow rate is calculated by the following modified expression:

$$Q_f = \frac{3600 \times P_w}{P_f \eta_p^{-1} - \left(P_f - P_{drop1} - P_{drop2}\right)(1 - R_1)(1 - R_2)Q_f \eta_{ERD}} \tag{40}$$

The simulation results are shown in Figure 10. In these simulations, selected values for water recovery in first stage (R_1) and a range of values for water recovery in second stage (R_2) were enforced. According to Figure 10, the overall recovery increases linearly with the second stage recovery, because the overall recovery is simply a function of R_1 and R_2, exclusively. At high values of R_2, the overall recovery for all values of R_1 converges to a high value. The growing global recovery reduces the recycled energy to the DWEER, which in turn reduces the water that can be produced by the wind-driven pump. This explains the degradation of feed flow rate as the recovery increases. As a result, the operating pressure increases to overcome the growing concentration polarization induced by the diminishing feed flow rate. It should be noted that the total recovery provides misleading information without inspecting the production rate. In fact, the permeate production increases linearly with R_2 with slower rate for the case of R_1 = 0.6. Nevertheless, the production rate for all cases converges at high R_2 to a value around 160 m³/h. The above behavior has its effect on the specific energy (i.e. total energy consumption per product flow rate). The specific energy for all cases decreases with increasing values of R_2, because of the increasing production rate at almost constant trans-membrane pressure. The specific energy reaches a minimum value of 0.35 kWh/m3 at recovery rate of 80%. For R_1= 0.3, the specific energy has a larger value at small R2 because at that specific low value of R_1 the production rate is lower than the other cases. The sketch of the salt concentration of the permeate in the second stage provides useful information. Considering that the salinity of potable water should be less than 0.5 kg/m³, the first stage should operate at a recovery ratio as high as 60% and that the recovery rate in the second stage should be in the range of $0.1 \le R_2 \le 0.6$. It is obvious that without an inter-stage pump, it is difficult to operate the second stage at high recoveries and acceptable water salinity. The situation is even worse, when the first stage is operating at high recovery rate. This is intuitive because operating the first stage at high recovery rate produces highly concentrated reject, which makes harder the operation of the second stage. The advantage of using two stages configuration is obvious. The production rate for all cases is higher than that obtained for a single stage system. Furthermore, the specific energy for all cases is less than 1 kWh/m3, which is also superior to what was observed for a single state configuration. The process performance at R_1 = 60% has a distinguished behavior compared to those at lower recovery values. It is evident from Figure 8 that the recovery rate of 50% presents an optimum and a turning point, where the RO performance afterward changes dramatically.
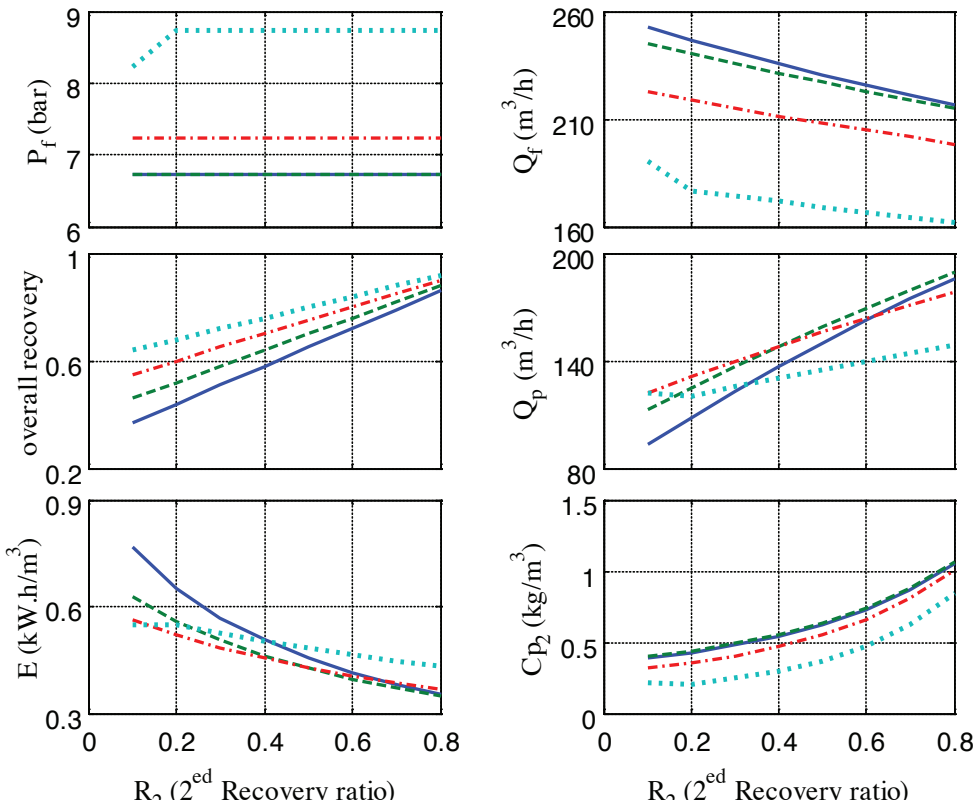
Fig. 10. Simulation of 2 stages RO system without booster pump, $\eta_P = 0.6$, $\eta_{ERD} = 0.9$, Cpd = 0.26 kg/m³; dotted: R_1=0.6; dash-dot: R_1=0.5; dashed: R_1=0.4; solid: R_1=0.3.

Two stage RO system with an inter-stage booster pump

The previous simulations confirmed the advantage of utilizing two consecutive stages of RO elements to benefit from the highly pressurized brine stream exiting the first stage. In fact, higher desalinate production and lower specific energy are observed. However, it was difficult to keep the salinity of the recovered water in the second stage below acceptable standards. The feed pressure of the second stage is fixed at a value lower than that of the main feed; in addition the feed salinity is more concentrated than that of the original brackish water. Therefore, attaining desired salt rejection and/or water recovery will be much harder. The situation could be worse, when high recovery is imposed in the first stage, because this will cut down the flow rate of the brine exiting the first stage and entering the second stage, which in turn deteriorates the second stage performance. It is well known that small RO feed flow increases membrane surface salt concentration and leads to the increase in the average osmotic pressure due to larger salt concentrations. Accordingly, it is of interest to add an inter-stage booster pump as shown in Figure 2. In common practice, the purpose of the booster pump is to help bring the makeup feed pressure to the desired main feed pressure. In our case, this issue can be handled by another approach as discussed earlier. Therefore, the function of the additional pump would be to adjust the performance specification of the second stage, e.g. the salinity of the final filtrate product. In due course, the salinity of the product in both stages are pre-

specified at 0.26 and 0.5 kg/m3, respectively. Hence, the problem is formulated as an optimization problem, i.e. determining the feed pressures, P_{f1} and P_{f2} that make the resulting product salinity meets the desired specifications for a given value for R_1 and R_2. The optimization problem is written as follows:

$$\min_{P_{f1},P_{f2}} \phi = P_{f1} + P_{f2}$$

Subject to

$$C_{p_1} \leq 0.26, \qquad C_{p2} \leq 0.5 \qquad 2 \leq P_{f1}, P_{f2} \leq 35 \tag{41}$$
$$f(x) = 0$$

In above expression, f represents the RO model Equations (11-28) with R1 and R2 being pre-specified. The optimization is solved numerically using MATLAB software. It should be noted that the main feed flow rate is computed using the following modified expression:

$$Q_f = \frac{3600 \times P_w}{P_{f1}\eta_p^{-1} - \left(P_{f2} - P_{drop2}\right)(1 - R_1)(1 - R_2)Q_f\eta_{ERD}} \tag{42}$$

Consequently, the specific energy should be calculated using the following:

$$E = \frac{Q_f P_{f1}\eta_p^{-1} + (P_{f2} - P_{c_1})Q_{c_1}\eta_p^{-1} - Q_{c_2}P_{c_2}\eta_{ERD}}{Q_p} \tag{43}$$

The result of the analysis is depicted in Figure 11. It can be seen that the optimization managed to maintain steady the values of Pf_1while increasing P_{f2} over the entire domain of R_2, for all selected capacity of the first RO stage. This behavior produced steady influent to the first stage. Consequently, the total distillate production grows with increasing R_2 until it reaches a maximum value of 180 m³/h. The total energy consumption per unit production presented a monotonically increasing trend for high R_1 (50-60%) and convex trend for lower R_1 (i.e. 30-40%).In fact, the specific energy can be as low as 0.45 kWh/m3for all cases of R1 within the range of $0.4 \leq R_2 \leq 0.6$ .The specific energy shown in Figure 11 has different trend for different R_1, some trends are in the form of monotone function and others in the form of convex function. As mentioned earlier, the specific energy depends on the feed pressure (P_{f1}, P_{f2}) and production rate (Q_p). Therefore, because Q_p and P_{f2} drifts are dissimilar for different R2, the corresponding specific energy trend is also different. The discrepancy in the specific energy trend among the different values for R_1 is attributed to the variation in the drifts of Q_p and P_{f2} over the R_2 domain. The figure also shows how the salinity of the second stage output is well maintained below the desired specifications. The interesting observation is the enhancement of the desalination process performance due to incorporation of a booster pump. This is evident as the distillate production is doubled and the required energy is still less than 1 kWh/m3. Moreover, the salinity of the product is within acceptable standards.
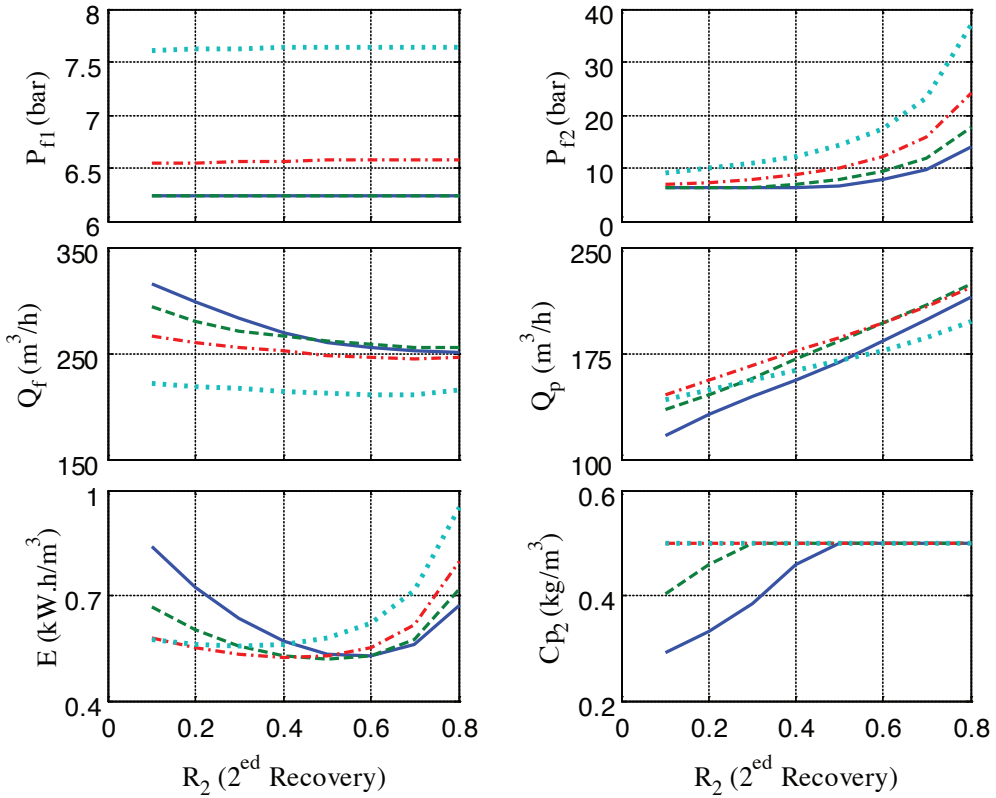
Fig. 11. Simulation of 2 stages RO system with inter-stage booster pump; $\eta_p = 0.6$, $\eta_{ERD} = 0.9$, C_{pd} = 0.26 kg/m^3; Cpd2 = 0.5 kg/m^3 dotted: R_1=0.6; dash-dot: R1=0.5; dashed: R_1=0.4; solid: R_1=0.3.

Effect of feed salinity

The results of Figure10 and 11 showed a variable performance for different values of R1. This is especially true for the specific energy (E). The minimum value of E and its location vary with R1 and R2. Therefore, it might be of interest to optimize the recovery ratio of both stages in order to achieve the optimum operating condition. The optimization problem can be written as follows:

$$\min_{R_1, R_2, P_{f_1}, P_{f_2}} E$$

Subject to

$$0.1 \le R_1, R_2 \le 0.8, \qquad 5 \le P_{f_1}, P_{f_2} \le 35$$

$$f(x) = 0$$

(44)

This optimization function consists of minimizing the specific energy for the RO system operation by identifying simultaneously the feed pressure and the recovery ratio of both stages. The optimization is constrained by the steady state RO model, i.e. the process mass balance and mass transfer phenomena. Moreover, the decision variables are constrained by their corresponding technical limits identified earlier, e.g. 80% for recovery rate and 35 bar for the feed pressure. The

outcome of the optimization is shown in Figure 12 for selected values of the feed concentration. The recovery rate of the first stage drops sharply with increasing feed salinity to keep the permeate salinity within the desired value. Conversely, the recovery rate for the second stage remains almost constant via the combinatorial effect of deceasing R1 and increasing Pf2. Thus, the overall recovery deceases with increasing feed salinity. As feed salinity increases, the osmotic pressure increases leading to a reduced mass flux through the membrane. Similarly, the pumping power needed to produce the desired water flux increases with increasing feed salinity. Consequently, the energy consumption increases due to additional hydrostatic pressure and diminishing production rate. The obtained overall recovery ranges from 53% to 75% for feed salt concentration ranging from 1 to 5 kg/m3. As comparison, Vincea et al. (2008) optimized their two-stage RO layout with salinity intake of 3kg/m3to reach an overall recovery rate of 82% with a recovery rate of 64% for the first stage and a recovery rate of 50% for the second stage. Our findings showed lower performance values than those reported by Vincea et al. (2008), because our optimization problem focused on minimizing the energy consumption. The optimal specific energy in our case is found to vary from 0.4 to 1.7 kWh/m3 over a salt concentration in the range of 1~5 kg/m3. Park et al. (2011), on the other hand, reported a minimum specific energy of 1.6~2.8 kWh/m3 for a brackish water salinity in the range of 2.75~5.5 kg/m3.
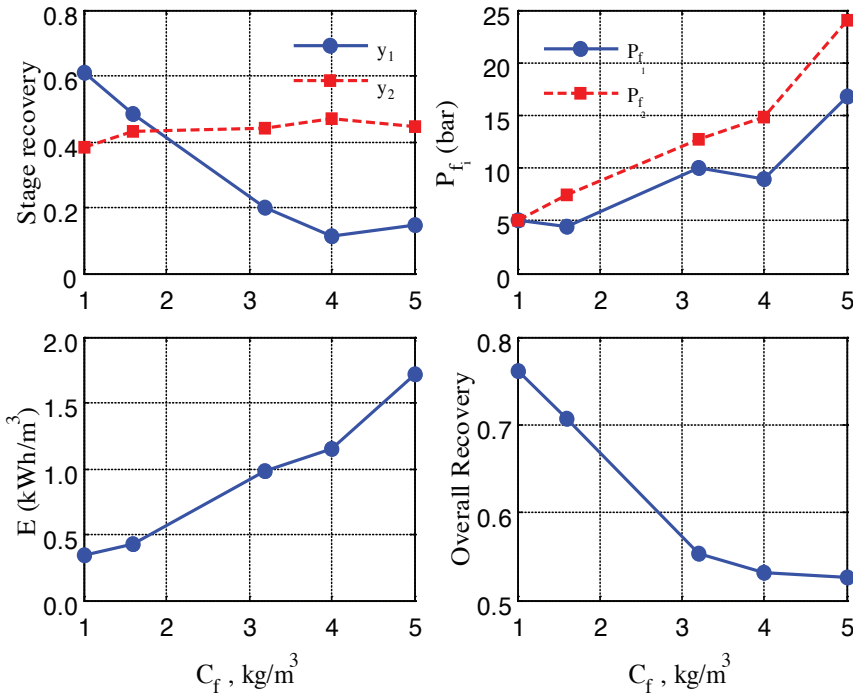
Fig. 12. Effect of feed concentration on optimal operation,

$\eta_p = 0.6$, $\eta_{ERD} = 0.9$, $C_{pd1} = 0.5$ kg/m³; $C_{pd2} = 0.5$ kg/m³

CONCLUSIONS

This investigation studied the potential utilization of wind energy in association with RO units in some arid areas of Saudi Arabia. It was found that the available wind power could be a viable energy source to power RO units for desalting brackish water. For a single stage RO unit, it was found that increasing the operating pressure generally leads to higher production rates and salt rejection, but limits the process throughput. Consequently, a certain maximum production rate may occur at specific recovery rates. The operation of two-stage RO system showed enhanced performance over a single stage in terms of production and energy consumption. The incorporation of an inter-stage booster pump positively improved the performance of the two-stage system. There is need to optimize the recovery ratio for high permeate flux and low energy consumption. The minimum specific energy for 1.6 g/l brackish water was found to be as low as 0.5 kWh/m^3 at a recovery ratio of 40~60% with a maximum production of 180 m^3/h. The analysis revealed that the best performance of the proposed process requires brackish water salinity to be less than 3 g/l. For higher values, the overall recovery rate decrease sharply and the specific energy increases rapidly.

ACKNOWLEDGEMENT

NOMENCLATURE

a	coefficient for pressure drop correlation
A_0	water permeability at 298K (m/h.bar)
A(T)	membrane permeability (m/h.bar)
B(T)	membrane solute permeability (m/h)
B_0	solute permeability at 298K (m/h)
b	coefficient for viscosity correlation
b_π	osmotic coefficient (m^3.bar/kg)
C	scale factor (m/s)
C_1	scale factor at 10m a.s.l (m/s)
C_2	scale factor at desired level (m/s)
CF	capacity factor
C_f, C_p, C_c	salt concentration in feed, permeate and brine (kg/m^3)
C_b, C_m	average salt concentration and salt concentration at membrane wall, (kg/m^3)
C_{pd}	desired salt concentration for permeate product, kg/m^3
D_{AB}	mass diffusivity (m^2/h)
d_h	hydraulic diameter of channel (m)
E	specific energy consumption (kwh/m^3)
Ep	feed pump energy (W)
E_{ERD}	recovered energy by ERD unit (W)
f(V)	Weibull probability density function
h_{sp}	height of spacer channel (m)
J_w	water flux (m/h)
J_s	salts mass flux (kg/m^2.h)

k	shape factor mass transfer coefficient (m/h)
k_1	shape factor at 10m a.s.
k_2	shape factor at desired level
k_s	mass transfer coefficient (m/h)
m, m_i	exponent in Eq. (2), molality of dissolved salt (ppm)
$\overline{P}, P_w$	average wind power (W)
P_R	rated-output power (W)
P_f, P_p, P_c	feed, permeate, and brine pressure (bar)
P_{drop}	pressure drop (bar)
$P(v)$	wind power function of wind velocity
Q_f, Q_p, Q_c	feed, permeate, and brine volumetric flow rate (m³/h)
Q_b	mean volumetric flow rate through membrane channel (m³/h)
R	recovery ratio (%)
Re	Reynolds number
SR	Salt rejection (%)
SP	Salt passage (%)
Sc	Schmidt number
Sh	Sherwood number
T, T_0	feed water and reference temperature (°C)
V	wind speed (m/s)
V_1, V_o, V_R	cut-in speed, cut-out speed, rated-output speed of wind, (m/s)
u	velocity of water in feed channel (m/h)
W	width of the membrane (m)
Z_0	roughness (m)
Z	geometric height (m)
Z_1	reference height (m)
Z_2	desired height (m)

Subscript

1,2	stage 1 and 2

Greek

α	coefficient for viscosity correlation and wind power correlation (Eq. 7)
β	coefficient for wind power correlation (Eq. 7)
γ	coefficient for wind power correlation (Eq. 7)
λ	coefficient for pressure drop correlation
π	osmotic pressure (bar)
μ, m_o	viscosity and reference viscosity (kg/m.s)
ε	Porosity
ν	Kinematic viscosity, (m²/h)
h_p, η_{ERD}	pump and DWEERefficiency

REFERENCES

Al-Bastaki, N. & Abbas, A. 2003. Permeate recycle to improve the performance of a spiral-wound RO plant. Desalination, **158**:119–26.

Agashichev, S.P. 2005. Reverse osmosis at elevated temperatures; influence of temperature on degree of concentration polarization and trans-membrane flux. Desalination, **179**:61–72.

Carta, J.A., Gonzhlez, J. & Subiela, V. 2004. The SDAWES project: an ambitious R&D prototype for wind powered desalination. Desalination, 161:33-48.

Charcosset, C. A. 2009. A review of membrane processes and renewable energies for desalination, Desalination, **245**(1-3):214-231

Chou, K.C. & Corotis, R.B. Simulation of hourly wind speed and array wind power, Solar Energy, **26**:199-212.

Clayton, M. E., Stillwill, A.S. & Webber, M.E. 2011. Implementation of brackish groundwater desalination using wind-generated electricity as a proxy for energy storage: a case study of the energy-water nexus in Texas. Proceeding of the 12ve International Mechanical Engineering Congress & Exposition, 11-17 November 2011, Colorado, United State.

Da Costa, A.R., Fane, A.G. & Wiley, D.E. 1994. Spacer characterization and pressure drop modelling in spacer-filled channels for ultrafiltration. Journal of Membrane Science, **87**:79–98.

Dashtpour, R. & Al-Zubaidy, S.N. 2012. Energy efficient reverse osmosis desalination process. International Journal of Environmental Science and Development, **4**:339-345.

DOW, 2006. Design a reverse osmosis system: design equations and parameters, Technical Manual,

Fath, H., Sadik, A. & Mezher, T. 2013. Present and future trend in the production and energy consumption of desalinated water in GCC countries. International Journal of Thermal and Environmental Engineering. **5**:155-65

Greenlee, L.F., Lawler, D.F., Freeman, B.D., Marrot, B & Moulin, P. 2009. Reverse osmosis desalination: Water sources, technology, and today's challenges. Water Research **43**:2317-48.

Justus C.G. & Mikhail, A. 1976. Height variation of wind speed and wind distributions statistics. Geophysics Research Letter, **3**:261–264.

Kaldellis, J.K., Kavadias, K. & Garofalakis, J. 2000. Renewable energy solution for clean water production in the Aegean archipelago islands. Mediterranean Conference on Policies and Strategies for Desalination and Renewable Energies, Santorini Island, Greece.

Khonkar, H., 2009. Complete Survey of Wind Behavior over the Arabian Gulf. Journal of King Abdulaziz University **20**(1):31-47.

Lagomarsino, S., Piccardo, G. & Solari, G. 1992. Statistical analysis of high return period wind speeds. Journal of Wind engineering and Industrial Aerodynamics, **41**: 485–496

Marriott, J, & Sorensen, E.A. 2003. A general approach to modelling membrane modules. Chemical Engineering Science **58**:4975–4990.

Martin, P.H. 1985. Wind power potential of Saudi Arabia, Solar and Wind Technology, **3**(2):139-142

Miranda, M.S. & Infield, D.A. 2002. A wind-powered seawater reverse-osmosis system without batteries. Desalination, **153**:9-16.

Park, G.L., Schafer, A.I. & Richards, B.S. 2011. Renewable energy powered membrane technology: The effect of wind speed fluctuations on the performance of a wind-powered membrane system for brackish water desalination. Journal of Membrane Science **370**:34–44.

Perry, R.H. & Green, D.W. 1985 Perry's chemical engineer's handbook. 6th ed. New York: McGraw-Hill.

Pestana, I. N., Latorre, F.J., Espinoza, C.A. & Gotor, A.G. 2004. Optimization of RO desalination systems powered by renewable energies. Part I: Wind energy. Desalination, **160**: 293-299.

Poje, S., & Cividini, B. 1988. Assessment of wind energy potential in Croatia. Solar Energy, **41**: 543–554.

Rautenbach, R. 1986. Process design and optimization. In: Bungay PM, Lonsdale HK, de Pinho MN, editors. Synthetic membranes: Science, Engineering and Applications. New York: Kluwer.

Rehman, S. 2006. Offshore wind power assessment on the east coast of Saudi Arabia. Wind Engineering, **29**:409-420.

Rehman S., Halwani, T.O. & Mohandes, M. 2003. Wind power cost assessment at twenty locations in the Kingdom of Saudi Arabia. Renewable Energy, **28**:573-583.

Sarkar P., Goswami, D., Prabhakar, S. & Tewari, P.K. 2008. Optimized design of a reverse osmosis system with a recycle. Desalination, **230**:128–139.

Sessions, B., Shih, W., MacHarg, J., Dundorf, S. & Arroyo, J. 2011. Optimizing brackish water reverse osmosis for affordable desalination. AMTA annual and SEDA annual, Miami Brach, FL, USA, 07-8.

Sherwood, T.K. & Brian, P.L.T., Fisher, R.E. 1967. Desalination by Reverse Osmosis. Industrial & Engineering Chemistry Fundamentals, **6**:2-12.

Sourirajan, S. 1970. Reverse osmosis. New York: Academic Press.

Srivathsan, G. 2013. Modeling of fluid flow in spiral wound reverse osmosis membranes. PhD dissertation, University of Minnesota.

Thomson, M., Miranda, M.S. & Infield, D. 2002. A small-scale seawater reverse-osmosis system with excellent energy efficiency over a wide operating range. Desalination, **153**:229–236.

Vince, F., Marechal, F., Aoustin, E. & Bréant, P. 2008. Multi-objective optimization of RO desalination plants. Desalination, **222**:96–118.

Vlachos, G. & Kaldellis, J.K. 2004. Application of a gas-turbine exhausted gases to brackish water desalination. A techno-economic evaluation. Applied Thermal Engineering, **24**: 2487–2500.

Wind-power-program.com. Wind turbine power curves. Available from: http://www.wind-power-program.com/turbine_characteristics.htm

Zejli, D., Aroui, K.E., Lazrak, A., Boury, K.E. & Elmidaoui, A. 2010. Economic feasibility of a 11-MW wind powered reverse osmosis desalination system in Morocco. Desalination and Water Treatment, **18**:164–174.

Zimmer, R. P., Justus, C. G., Mason, R. M., Robinette, S. L., Sassone, P. G. & Schalter, W. A. 1975. Benefit-cost methodology study with example application of the use of wind generators. NASA CR-134864.